Shear rheology of graphene oxide dispersions

Francesco Del Giudice[a,], Amy Q. Shen[a]

[a]*Micro/Bio/Nanofluidics Unit, Okinawa Institute of Science and Technology Graduate University, Japan.*

Abstract

Graphene oxide (G-O) is a chemically oxidized sheet of graphene. Due to their functional groups, G-O sheets have found numerous applications in biomedical, electrical and material engineering. The flow properties of G-O dispersions, i.e., the *rheology*, are intimately related to the material processing and design of G-O based composites. In this review, we report recent findings on the shear rheology of both aqueous G-O dispersions and composite materials containing G-O sheets. We focus on aqueous G-O dispersions to understand interactions between G-O sheets. Applications related to materials science and technology are also presented.

1. Introduction

Around 10 years ago, the experimental isolation of the first single sheet of graphene [1, 2], a 2-dimensional monolayer of carbon atoms, raised great excitement in the material science community, because its physical existence had been debated for 70 years [3]. Since then graphene has been considered as a "rising star", and countless applications have been introduced. Many of these are related to a chemically modified version of graphene, called graphene oxide (G-O). In particular, G-O contains a variety of reactive oxygen functional groups, making it versatile through different chemical modifications [4]. Due to their excellent mechanical, thermal, and electric properties, G-O sheets have been used in various applications such as nanocomposites [5], inks [6], and coating for supercapacitor electrodes [7, 8]. Rheology of G-O dispersions depends on parameters such as G-O concentration and sheet size, which are critical for the design of *ad-hoc* materials. When dispersed, G-O sheets tend to aggregate [9, 10, 11], similar to suspensions containing carbon nanotubes [12] or rod-like micelles [13], because attractive forces are dominant. Despite the extensive literature in the rheology of carbon nanotube based materials (both in dispersion [14] and composite [15] forms), much less has been reported on the rheology of graphene oxide dispersions.

In this review, we focus on existing findings on the shear rheology of aqueous G-O dispersions and G-O-composites. Due to space limitations, results for G-O interfacial rheology can be found in Imperiali *et al.* [16], G-O electorheology is reviewed by Zhang *et al.* [7]. We also refer to the review of Fan *et al.* [17] for

*Amy Q. Shen

Email address: amy.shen@oist.jp (Amy Q. Shen)

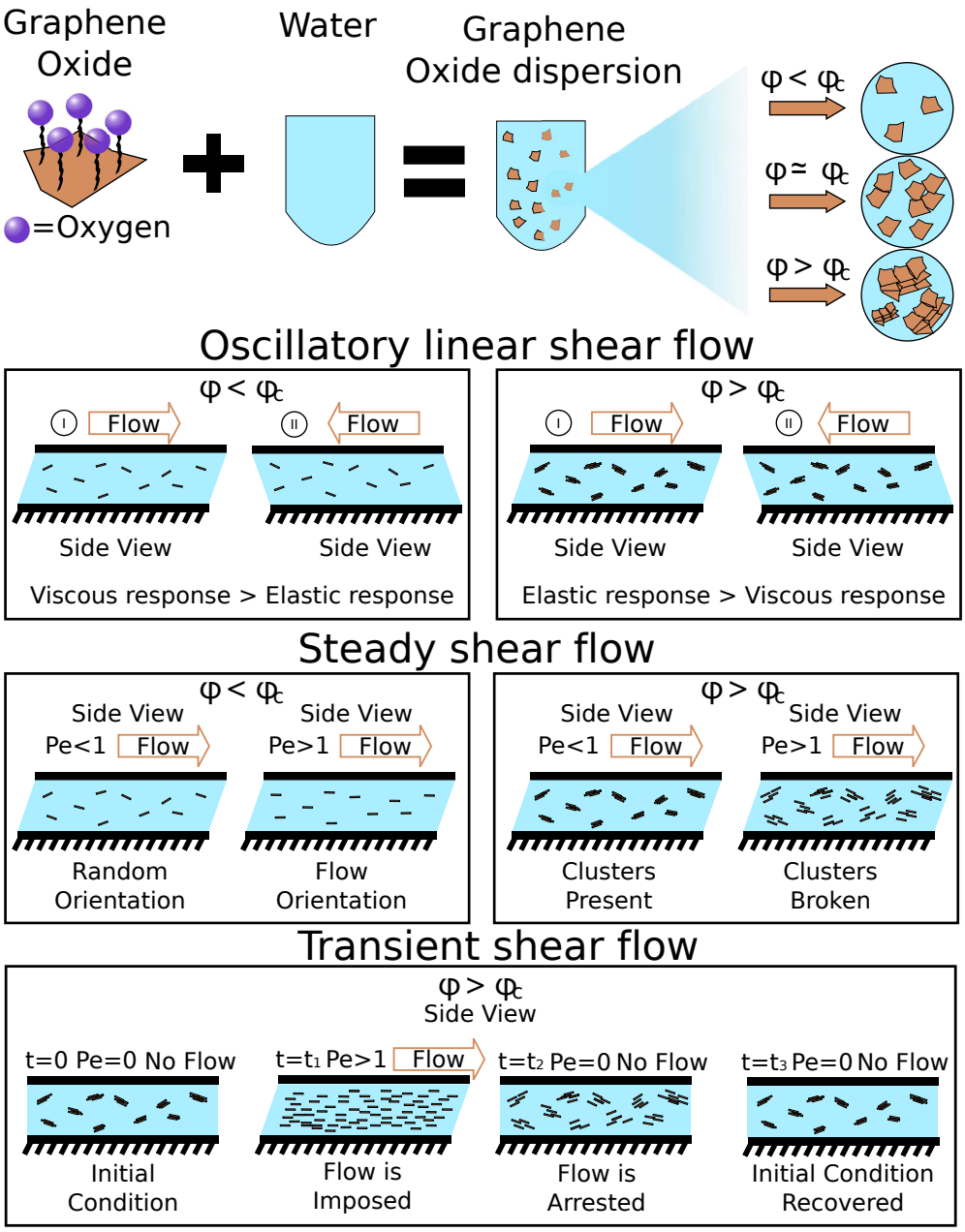

Figure 1: G-O aqueous dispersions at different volume concentrations ϕ are prepared by adding G-O in water. **Oscillatory linear shear flow:** When $\phi < \phi_c$ (ϕ_c is the critical volume or mass concentration) viscous response due to the drag of the G-O sheets prevails over the elastic response. When $\phi > \phi_c$ elastic response due to the G-O self-aggregation prevails over the viscous response due to the drag of the clusters. **Steady shear flow:** When $\phi < \phi_c$ and at Peclet number $Pe = \dot{\gamma}a^2/D_0 < 1$, where $\dot{\gamma}$ is the applied shear rate, a is the average sheet radius, and D_0 is the sheet diffusivity, G-O sheets are randomly oriented; while at $Pe > 1$ G-O sheets are oriented along the flow direction. When $\phi > \phi_c$ and at Peclet number $Pe < 1$, G-O are arranged in randomly oriented clusters; while at $Pe > 1$ clusters are broken down. **Transient shear flow:** Only the case $\phi > \phi_c$ is considered. Initially, the dispersion is arranged in randomly oriented clusters. After applying a flow at $Pe > 1$, clusters are broken down and G-O sheets are oriented along the flow direction. When the flow is arrested, $Pe = 0$, G-O sheets start to self-arrange. After sufficient resting time, G-O sheets recover the initial cluster configuration.

energy-related applications of G-O sheets.

2. Shear rheology of aqueous graphene oxide dispersions

Shear rheological characterization is generally fulfilled through measurements in *oscillatory linear shear flow*, *steady shear flow* and *transient shear flow*. We have organized this review into sections based on flow types, in the order commonly adopted to describe G-O rheology. A schematic representation of the findings is summarized in Figure 1.

2.1. Oscillatory linear flow properties

In oscillatory shear flow, a sinusoidal small deformation is applied, and the response of the material is measured in terms of elastic modulus G' and viscous modulus G'' [18]. From these measurements, important information on the local conformation of G-O sheets in dispersion can be derived. Naficy *et al.* [9] recently presented interesting results on the relationship between morphology and both G' and G'' of G-O dispersions (Figure 2a-c). At concentration $c = 0.05$ mg/ml, they found that both G' and G'' were frequency dependent, in agreement with other reports [10, 11]. By increasing the concentration to $c = 0.5$ mg/ml (Figure 2b), interactions between G-O sheets cause stronger elastic responses than viscous responses in the G-O dispersion. At concentration $c = 4.5$ mg/ml, the two moduli are almost frequency independent (similar to the gel response [18]), with G-O sheets being packed in superimposed layers. These findings reveal the existence of a *critical concentration* ϕ_c, above which G-O sheets aggregate, due to Brownian diffusion. Naficy *et al.* [9] found a critical concentration $\phi_c = 0.22$ mg/ml, and studied G-O dispersions in the range $0.2 < \phi/\phi_c < 60$. The transition between dispersed G-O sheets at low concentrations to ordered clusters at high concentrations is similar to the transition from isotropic to nematic phase in *liquid crystals* [19]. Such behavior is mainly caused by the high aspect ratio of G-O sheets, which also affects the value of the critical concentration ϕ_c [20]. Elastic and viscous response in oscillatory flow is also in agreement with that of semi-dilute ($\phi/\phi_c > 1$) aqueous carbon nanotube dispersions [14], where G' and G'' display the same response as shown in Figure 2.

More detailed rheological characterizations of G' and G'' have been carried out by Vasu *et al.* [11] at concentrations $0.27 < \phi/\phi_c < 80$ (with $\phi_c = 0.038$ vol%), and by Vallés *et al.* [10] at concentrations $1 < \phi/\phi_c < 267$ (with $\phi_c = 0.033$ vol%). Interestingly, Vasu *et al.* [11] derived ϕ_c by examining the dependence of the elastic modulus G', at low strains and amplitudes, as a function of ϕ. They obtained $\phi_c = 0.038$ vol%, which is in good agreement with $\phi_{c,theo} = 0.040$ vol% based on the theory of geometrical percolation thresholds for randomly oriented thin-disks [21]. At $\phi/\phi_c < 1$ G-O sheets are randomly distributed, but aggregated in more ordered structures at $\phi/\phi_c > 1$.

2.2. Steady shear flow properties

While oscillatory shear flow properties are related to small and linear deformations, steady shear properties are related to non-linear high deformations [18].

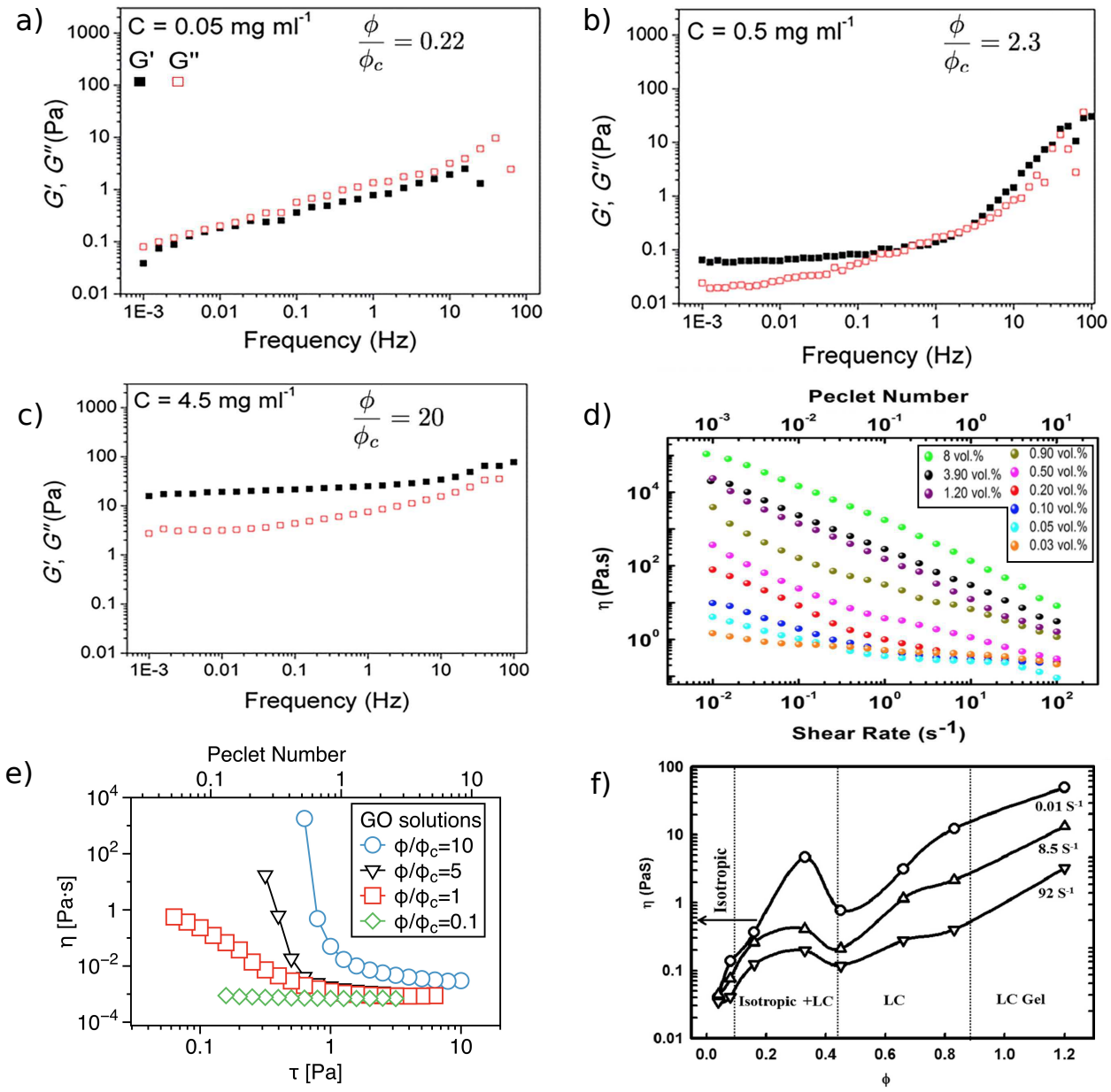

Figure 2: Elastic modulus G' and viscous modulus G'' of aqueous G-O dispersions as a function of the frequency at a) c = 0.05 mg/ml, b) c = 0.5 mg/ml, c) c = 4.5 mg/ml (ϕ_c = 0.22 mg/ml). Adapted from Naficy *et al.* [9] with the permission of The Royal Society of Chemistry. d) Steady shear viscosity η as a function of the shear rate $\dot{\gamma}$ for G-O dispersions at different concentrations (ϕ_c = 0.03 vol%). The top axis shows the Peclet number Pe. Adapted from Vallés *et al.* [10]. e) Steady shear viscosity η as a function of the shear stress τ for G-O dispersions at different concentrations (ϕ_c = 0.04 wt%). The top axis shows the Peclet number Pe. Experiments are performed in a stress-controlled rheometer with a parallel glass plate configuration (with 43 mm in diameter, gap size of 200 μm). Del Giudice *et al.* (IMN Del Giudice *et al.*, unpublished). f) Shear viscosity η at fixed shear rate $\dot{\gamma}$ as a function of the G-O volume concentration ϕ (ϕ_c = 0.33 vol%). Reprinted from *Carbon*, Vol.80, Kumar *et al.*, Rheological properties of graphene oxide liquid crystal, pages 453-461, Copyright (2014) with permission from Elsevier [22].

In Figure 2d the shear viscosity η is plotted as a function of the shear rate $\dot{\gamma}$, for G-O dispersions at $1 < \phi/\phi_c < 267$ (with ϕ_c = 0.033 vol%) [10]. At concentrations $\phi/\phi_c \leq 2$ (i.e., $\phi \leq 0.05$ vol%) and shear rate

$\dot{\gamma} > 1\ s^{-1}$, η remains as a constant; while at $\dot{\gamma} < 1\ s^{-1}$, η decreases with increasing $\dot{\gamma}$, showing the so called *shear-thinning* behavior. At concentrations $\phi/\phi_c \geqslant 2$ (i.e., $\phi \geqslant 0.05$ vol%), the shear-thinning becomes more pronounced with increasing ϕ. Such response implies the existence of a *yield stress* in the G-O dispersion, i.e., the lowest stress required to induce the flow. Yield stress for G-O dispersions at $\phi/\phi_c > 1$ has also been reported elsewhere [9, 11, 19].

G-O sheets at $\phi/\phi_c > 1$ aggregate (Figure 2(b-c)) because of Brownian diffusion. However, if the applied deformation increases, the aggregates become disassociated by the flow, i.e., convection overcomes diffusion. Note that similar aggregation mechanism has been reported to lead to the gelation of rod-like micelles [13], where the effects of convection and diffusion are quantified by the Peclet number Pe, described as [23]:

$$Pe = \frac{\dot{\gamma} a^2}{D_0}, \tag{1}$$

where $\dot{\gamma}$ is the applied shear rate, a is the average sheet radius, and D_0 is the sheet diffusivity. When $Pe < 1$, diffusion overcomes convection, and vice versa when $Pe > 1$. Values of the Peclet number are reported on the top axis of Figure 2d. An increase in the shear rate leads to an increase in convection, hence an increase in Pe. As a consequence, G-O sheets do not aggregate, but are dispersed and aligned with the flow direction. Since the drag generated by an oriented sheet is much smaller than that generated by a cluster, the shear viscosity decreases up to a constant value (when all sheets are aligned with the flow). When the shear flow is arrested, $Pe = 0$, G-O sheets would diffuse and self-arrange, as observed in *thixotropic* materials[1].

It is not possible to directly derive the yield stress τ_y from Figure 2d. This important property can be determined simply by examining the steady shear viscosity η as a function of the imposed shear stress τ (Figure 2e) (IMN Del Giudice *et al.*, unpublished). We observe two distinct zones, one at $\tau > 3$ Pa ($\dot{\gamma} \sim 10^3\ s^{-1}$), for all the G-O concentrations, where the viscosity is constant and equal to that of the water (solvent of the dispersion). Another zone at lower stresses and at $\phi/\phi_c = 0.1$ (with $\phi_c \sim 0.04$ wt%), where η exhibits the shear-thinning behavior (Figure 2d). We also show comparisons in the Peclet number dependency (Figure 2e). We find $\tau_y = 0.7\ Pa, \tau_y = 0.3\ Pa, \tau_y = 0.1$ Pa, for $\phi/\phi_c = 10$, $\phi/\phi_c = 5$, $\phi/\phi_c = 1$, respectively, in good agreement with those reported elsewhere [11].

Figure 2(d-e) show that the shear viscosity at a fixed $\dot{\gamma}$ increases monotonically with the concentration ϕ in the range of $1 < \phi/\phi_c < 267$. Kumar *et al.* [22] (Figure 2f) observed a non-monotonic behavior of the shear viscosity at a fixed shear rate when increasing the volume concentration of the G-O dispersion, when $0.6 < \phi/\phi_c < 1.2$ (with ϕ_c =0.33 vol%). They attributed such behavior to the transition from isotropic to nematic phase in the G-O dispersion, around ϕ_c. Notice that their reported ϕ_c differs of one order of magnitude from those of Vasu *et al.* ($\phi_c = 0.038$ vol%) [11] and Vallés *et al.* ($\phi_c = 0.033$ vol%) [10]. Future experimental works are needed to study the occurrence of such transitions by expanding the range of

[1] According to the definition of Barnes, Hutton and Walters [24], *thixotropy* (verbatim) "is the decrease (in time) of ... viscosity under constant shear stress or shear rate, followed by a gradual recovery when the stress or shear rate is removed."

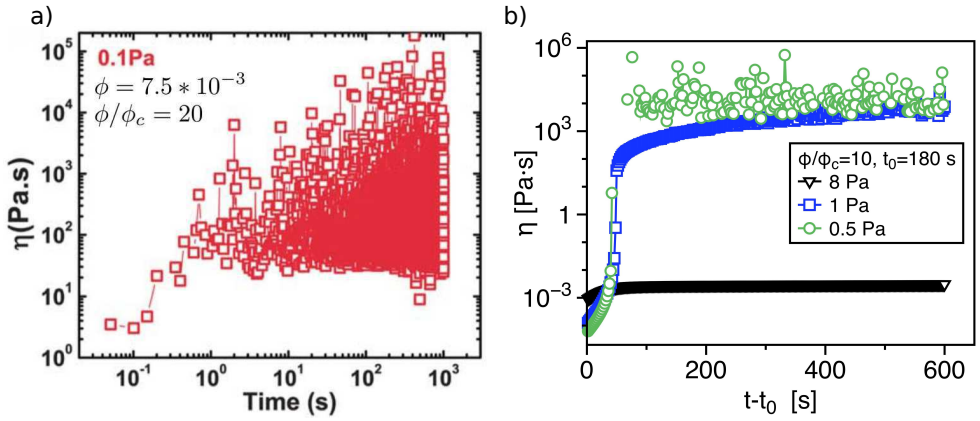

Figure 3: a) Shear viscosity as a function of time for a G-O dispersion with $\phi = 0.75$ wt% with an imposed shear stress $\tau = 0.1$ Pa. Yield stress at $\phi/\phi_c = 20$ ($\phi_c = 0.038$ vol%) is $\tau_y = 1$ Pa. Adapted from Vasu *et al.* [11] with permission from The Royal Society of Chemistry. b) Shear viscosity as a function of time for a G-O dispersion at $\phi/\phi_c = 10$ ($\phi_c \sim 0.4$ wt%), with $t_0 = 180$ s of preshear time at τ =20 Pa, for several imposed shear stress τ. Yield stress for $\phi/\phi_c = 10$ is $\tau_{y,0.4} = 0.7$ Pa. Experiments are performed in a stress-controlled rheometer with a steel parallel plate configuration (50 mm in diameter, gap size of 200 μm). Data obtained from Del Giudice *et al.* (IMN Del Giudice *et al.*, unpublished).

concentrations investigated over the interval $0.6 < \phi/\phi_c < 1.2$.

Tesfai *et al.* [25] studied G-O solutions in the range $0.005 < c < 0.05$ wt% (they did not provide an estimate of ϕ_c). They reported a weak shear thinning at $\dot{\gamma} < 100\ s^{-1}$ for concentrations $c > 0.03$ wt%, and the zero-shear viscosity η_0 increases with the increasing concentration.

2.3. Transient shear flow properties

Thixotropic materials such as aqueous G-O dispersions, strongly depend on the flow history [26]; hence time dependent measurements are very important to fully understand their properties. In addition, controlling the shear history before starting the actual measurement is crucial. Comparisons between dispersions at different concentrations cannot be reliably made, unless the same *initial measurement conditions* are uniformly applied to all samples, prior to each measurement. For instance, preliminary uniform shear (*preshear*), or preliminary long resting time are two options to achieve the measurement consistency.

Despite their importance, very few studies [11, 10, 27] have considered transient rheological experiments, and only few results were presented. Liu *et al.* [27] reported transient viscosity for G-O dispersions with $0.75 < \phi/\phi_c < 3$ (with ϕ_c =0.8 wt%), at a fixed shear rate $\dot{\gamma} = 100\ s^{-1}$ for a measurement duration of 120 s, without applying any preshear or resting time. They found that a clear steady state was never reached, but measurements longer than 120 s are unfortunately not available. Vasu *et al.* reported that shear viscosity η displays strong fluctuations as a function of time for an imposed shear stress $\tau = 0.1\ Pa$ ($< \tau_y = 1\ Pa$), at a fixed $\phi/\phi_c = 20$ (Figure 3a). In Figure 3b (IMN Del Giudice *et al.*, unpublished), the transient viscosity for different applied stresses is displayed, for G-O dispersions with $\phi/\phi_c = 10$. A preshear of $\tau = 20$ Pa for $t_0 = 180$ s has been applied before each measurement. At $\tau > \tau_y = 0.7\ Pa$, shear viscosity reaches a

steady-state in less than 100 s. When approaching the yield stress τ_y from $\tau > \tau_y$, viscosity exhibits some small fluctuations (at $\tau = 1$ Pa), but strong fluctuations emerge when $\tau = 0.5\ Pa < \tau_y$, in agreement with the results of Figure 3a. Notice that at $\tau = 0.5$ Pa, some data points are not connected by lines, because the rheometer detects some negative values, confirming the existence of the yield stress, also reported by Vasu *et al.* [11]. The increase of transient viscosity at low imposed shear (i.e., below the yield stress) is also common in carbon nanotube suspensions [12, 28].

3. Shear rheology G-O composites

Graphene oxide has been widely used to improve mechanical properties of a variety of materials, such as polydimethylsiloxane (PDMS) [29, 30, 31], hydrogels [32, 33, 34, 35], polycarbonate [5, 36], polymethyl methacrylate [37], polyurethane [38], and cellulose [39]. El Achaby and Qaiss [40] compared the rheological behavior of polyethylene filled with G-O and carbon nanotubes. They found that at the same filler concentration, G-O sheets performed better than carbon nanotubes in terms of rheological, thermal, and tensile properties, due to higher specific surface area of G-O sheets. Jalili *et al.* [41] used G-O dispersions at $\phi > \phi_c$ to produce long and 'ultrastrong' fibers with diameters down to $\sim$30 μm. Very recently, G-O sheets have been used to form ternary composite materials. For instance, Nasab and Kalaee [42] used epoxy resin mixed with 0.1 wt% of graphene oxide, with different amounts of liquid polysulfide. The resulting material showed elastic modulus up to 10^9 Pa, and solved the common drawback of brittleness associated with epoxy resins.

Because of space limitations, we now focus our attention on PDMS and hydrogels related G-O composites, because of their wide use, ranging from biomedical engineering to materials science. Niu *et al.* [30] studied the effect of G-O addition on PDMS with two different molecular weights M_w. They found that at G-O concentrations well above the critical concentration, sheets are ordered. On the other hand, in proximity to the critical concentration, ordering is found only in low molecular weight PDMS. This phenomenon is not yet understood. The same authors studied the effect of G-O surface chemistry on the rheology of the composite materials [31]. This study shows negative values of the difference[2] between the two *normal stress difference* ($\Delta N = N_1 - N_2$) as a function of the shear rate, because of sheet aggregation. Comparisons with other carbon-based materials [12] suggest that the alignment of G-O sheets along the vorticity direction, also called *vorticity banding* [43] can lead to negative ΔN. Further investigations are still required.

Graphene oxide has also been reported to enhance the polymer cross-linking process in hydrogels [32, 33, 35]. Liu *et al.* [32] prepared two types of hydrogels, one made of unmodified poly-isopropylacrylamide copolymer (P3), and another made of the same copolymer modified with G-O sheets (HGIC-3). They then analyzed the gelation temperature T_{gel} of the two hydrogels, by monitoring G' and G'' at fixed angular

[2]There are two normal stress differences usually defined in rheology, namely the first normal stress difference $N_1 = \tau_{xx} - \tau_{yy}$ and the second normal stress difference $N_2 = \tau_{yy} - \tau_{zz}$, where τ_{xx}, τ_{yy} and τ_{zz} are the stresses normal to the flow direction, gradient direction, and vorticity direction, respectively [18].

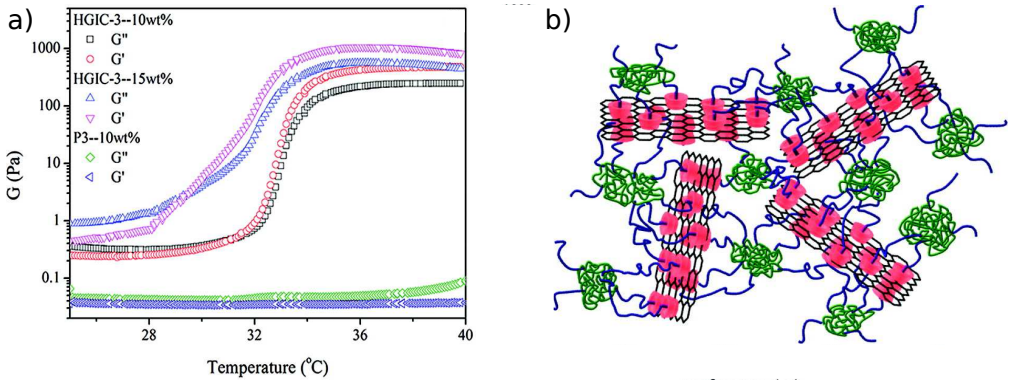

Figure 4: (a) Elastic modulus G' and viscous modulus G'' as a function of the temperature for different hydrogels. P3 is the unmodified hydrogel with 10 wt% of copolymer. HGIC-3 are the hydrogels obtained from the copolymer modified with G-O addiction at 10 wt% and 15 wt%. (b) Schematic of the possible HGIC structure, where G-O sheets are represented in red, polymer chains in green, and cross-links in blue. Reprinted from J. Liu *et al.*, Supramolecular hybrid hydrogels from noncovalently functionalized graphene with block copolymers, *Macromolecules*, 44(19), (2011), pages 7682-7691 [32], with permission from American Chemical Society.

frequency $\omega = 1$ Hz as a function of the temperature[3]. They found that G' and G'' of the P3 hydrogel are independent of the temperature up to $T = 40°$C; thus, no gelation temperature can be identified. The HGIC-3 hydrogel, instead, shows a clear dependence of the two moduli at low temperatures, with a gelation temperature $30°C < T_{gel} < 35°C$ for HGIC-3 samples (Figure 4a). The authors suggest that G-O sheets enable polymer cross-linking and promote connectivity within the composite solution (see Figure 4b). Similar findings were reported by Das *et al.* [33]. Kim and Lee also studied the effect of G-O sheets on hydrogel composite rheology [34], reporting that oscillatory flow promote gelation only at deformation $\gamma < 20$ %. Bai *et al.* [35] showed that the addition of cross-linkers (polymers, metal ions, and ammonium salts) or the acidification of G-O aqueous solutions above ϕ_c led to G-O gelation, with a consequent formation of (verbatim) "super" and "smart" G-O hydrogels. Tan *et al.* [44] added small amount of G-O to polyvinyl alcohol (PVA) solutions to produce uniformly sized fibers with an average diameter of ~ 200 nm, through electrospinning. The orientation of G-O sheets promotes the stretching of PVA chains, leading to uniform distribution of fiber diameters.

4. Conclusions and Outlook

In this review, the rheology of aqueous and composite graphene oxide dispersion is presented. The shear rheology of G-O dispersion can be summarized as follows. (i) A critical concentration ϕ_c exists, below which G-O sheets are dispersed, and above which they self-organize. (ii) At $\phi/\phi_c > 1$, G-O aggregates are formed or dismantled, depending upon wether the dominant mechanism is Brownian diffusion or flow convection,

[3]We recall here that T_{gel} can be derived from measures of G' as function of the temperature. T_{gel} is evaluated as the temperature at which G' reaches a plateau after experiencing an increase in its value, as in the case of HGIC-3 (Figure 4a).

quantified by the Peclet number. At low Pe, G-O sheets self-aggregate, while at high Pe such aggregates disassociate. (iii) G-O aggregates are reversibly formed once the flow is arrested; thus G-O dispersions act as thixotropic fluids. Regarding composites, G-O sheets significantly increase the elastic and viscous modulus of the composite materials, and simplify the cross-linking process between polymer chains.

For the transient rheology of G-O systems, available data are either scarce or incomplete, and the comparisons between steady state and transient measurements over long time scales require further investigations. In addition, the nature of a negative normal stress differences in G-O dispersions is still not fully understood. Finally, the rheological characterization of G-O dispersions in extensional flows deserves a special mention, because only one recent work [45] is available in literature, where the extensional viscosity of a polyvinyl chloride/G-O (PVC/GO) composite was found to be up to three orders of magnitude larger than that of simple PVC.

New outlooks in G-O dispersions arise from investigating the rheology of modified aqueous G-O dispersions due to salt [46] or polyethylene glycol [47] additives, in order to manipulate interactions between the G-O sheets.

From a technological point of view, there is great potential to employ microfluidics to encapsulate and polymerize G-O dispersions to create spongy particles for oil absorption [48]. Technologies for synthesis of G-O dispersions in Taylor-Couette flow also grant further investigation since they are easy to operate with scale-up potential [49, 50].

Exceptional properties of graphene oxide are pushing research and industry to develop new technologies, making the G-O market the largest segment of the graphene business. Novel applications in the field of health care are also expected, for example in the production of G-O based biosensors for disease detection [51, 52].

5. Aknowledgements

The authors thank prof. Pier Luca Maffettone for helpful discussion and comments. The authors thank also Dr. Steve Aird for careful proof reading.

References

[1] K. S. Novoselov, A. K. Geim, S. V. Morozov, D. Jiang, Y. Zhang, S. V. Dubonos, I. V. Grigorieva, A. A. Firsov, Electric field effect in atomically thin carbon films, Science 306 (5696) (2004) 666–669.

[2] A. K. Geim, K. S. Novoselov, The rise of graphene, Nat Mater 6 (3) (2007) 183–191.

[3] L. D. Landau, Zur theorie der phasenumwandlungen ii, Phys Z Sowjetunion 11 (1937) 26–35.

[4] D. R. Dreyer, S. Park, C. W. Bielawski, R. S. Ruoff, The chemistry of graphene oxide, Chem Soc Rev 39 (1) (2010) 228–240.

[5] J. R. Potts, D. R. Dreyer, C. W. Bielawski, R. S. Ruoff, Graphene-based polymer nanocomposites, Polymer 52 (1) (2011) 5–25.

[6] Q. Mei, Z. Zhang, Photoluminescent graphene oxide ink to print sensors onto microporous membranes for versatile visualization bioassays, Angew Chem Int Edit 51 (23) (2012) 5602–5606.

[7] J. Zhang, X. Zhao, Conducting polymers directly coated on reduced graphene oxide sheets as high-performance supercapacitor electrodes, J Phys Chem 116 (9) (2012) 5420–5426.

[8] Y. Su, S. Li, D. Wu, F. Zhang, H. Liang, P. Gao, C. Cheng, X. Feng, Two-dimensional carbon-coated graphene/metal oxide hybrids for enhanced lithium storage, ACS Nano 6 (9) (2012) 8349–8356.

[9] S. Naficy, R. Jalili, S. H. Aboutalebi, R. A. Gorkin III, K. Konstantinov, P. C. Innis, G. M. Spinks, P. Poulin, G. G. Wallace, Graphene oxide dispersions: tuning rheology to enable fabrication, Mater Horiz 1 (3) (2014) 326–331.

[10] C. Vallés, R. J. Young, D. J. Lomax, I. A. Kinloch, The rheological behaviour of concentrated dispersions of graphene oxide, J Mater Sci 49 (18) (2014) 6311–6320.

[11] K. Vasu, R. Krishnaswamy, S. Sampath, A. Sood, Yield stress, thixotropy and shear banding in a dilute aqueous suspension of few layer graphene oxide platelets, Soft Matter 9 (25) (2013) 5874–5882.
••This article reports the most comprehensive rheological characterization of graphene oxide dispersions at $0.27 < \phi/\phi_c < 80$ (with $\phi_c = 0.038$ vol%) in oscillatory, steady-shear, transient shear and Couette flow.

[12] S. Lin-Gibson, J. Pathak, E. Grulke, H. Wang, E. Hobbie, Elastic flow instability in nanotube suspensions, Phys Rev Lett 92 (4) (2004) 048302.

[13] R. Bruinsma, W. M. Gelbart, A. Ben-Shaul, Flow-induced gelation of living (micellar) polymers, J Chem Phys 96 (10) (1992) 7710–7727.

[14] E. K. Hobbie, Shear rheology of carbon nanotube suspensions, Rheol Acta 49 (4) (2010) 323–334.

[15] T. Chatterjee, R. Krishnamoorti, Rheology of polymer carbon nanotubes composites, Soft Matter 9 (40) (2013) 9515–9529.

[16] L. Imperiali, K.-H. Liao, C. Clasen, J. Fransaer, C. W. Macosko, J. Vermant, Interfacial rheology and structure of tiled graphene oxide sheets, Langmuir 28 (21) (2012) 7990–8000.

[17] X. Fan, D. W. Chang, X. Chen, J.-B. Baek, L. Dai, Functionalized graphene nanoplatelets from ball milling for energy applications, Curr Opin Chem Eng 11 (2016) 52–58.

[18] C. Macosko, Rheology: Principles, measurements, and applications. 1994, Wiley-VCH, 1994.

[19] Z. Xu, C. Gao, Aqueous liquid crystals of graphene oxide, ACS Nano 5 (4) (2011) 2908–2915.

[20] X. Yang, C. Guo, L. Ji, Y. Li, Y. Tu, Liquid crystalline and shear-induced properties of an aqueous solution of graphene oxide sheets, Langmuir 29 (25) (2013) 8103–8107.

[21] M. Sahimi, S. Arbabi, Mechanics of disordered solids. ii. percolation on elastic networks with bond-bending forces, Phys Rev B 47 (2) (1993) 703.

[22] P. Kumar, U. N. Maiti, K. E. Lee, S. O. Kim, Rheological properties of graphene oxide liquid crystal, Carbon 80 (2014) 453–461.

[23] N. J. Wagner, J. F. Brady, Shear thickening in colloidal dispersions, Phys Today 62 (10) (2009) 27–32.

[24] H. A. Barnes, J. F. Hutton, K. Walters, An introduction to rheology, Vol. 3, Elsevier, 1989.

[25] W. Tesfai, P. Singh, Y. Shatilla, M. Z. Iqbal, A. A. Abdala, Rheology and microstructure of dilute graphene oxide suspension, J Nanopart Res 15 (10) (2013) 1–7.

[26] H. A. Barnes, Thixotropy—a review, J Non-Newton Fluid 70 (1) (1997) 1–33.

[27] Y. Liu, C. Chen, L. Liu, G. Zhu, Q. Kong, R. Hao, W. Tan, Rheological behavior of high concentrated dispersions of graphite oxide, Soft Matter 13 (3) (2015) 167–175.

[28] G. Natale, G. Ausias, J. Férec, M. Heuzey, P. Carreau, Modeling interactions in carbon nanotube suspensions: Transient shear flow, J Rheol 60 (6) (2016) 1069–1083.

[29] A. Guimont, E. Beyou, G. Martin, P. Sonntag, P. Cassagnau, Viscoelasticity of graphite oxide-based suspensions in pdms, Macromolecules 44 (10) (2011) 3893–3900.

[30] R. Niu, J. Gong, D. Xu, T. Tang, Z.-Y. Sun, Influence of molecular weight of polymer matrix on the structure and rheological properties of graphene oxide/polydimethylsiloxane composites, Polymer 55 (21) (2014) 5445–5453.

••This article performs a detailed rheological characterization of graphene oxide-PDMS composites, to understand the surface chemistry effect on the vorticity banding instability. The authors show that intra-attractive interactions seem to be responsible for the negative first normal stress difference and consequently lead to the vorticity banding.

[31] X. Niu, J. Gong, D. Xu, T. Tanga, Z.-Y. Sun, Impact of particle surface chemistry on the structure and rheological properties of graphene-based particle/polydimethylsiloxane composites, RSC Adv 5 (2015) 34885–34893.

[32] J. Liu, G. Chen, M. Jiang, Supramolecular hybrid hydrogels from noncovalently functionalized graphene with block copolymers, Macromolecules 44 (19) (2011) 7682–7691.

• This article shows that graphene oxide in hydrogel composites simplify the crosslink process of polymers, possibly induced by the spatial orientation and the high aspect ratio of G-O sheets.

[33] S. Das, F. Irin, L. Ma, S. K. Bhattacharia, R. C. Hedden, M. J. Green, Rheology and morphology of pristine graphene/polyacrylamide gels, ACS Appl Mater Interfaces 5 (17) (2013) 8633–8640.

[34] J. E. Kim, H. S. Lee, Oscillatory shear induced gelation of graphene–poly (vinyl alcohol) composite hydrogels and rheological premonitor of ultra-light aerogels, Polymer 55 (1) (2014) 287–294.

[35] H. Bai, C. Li, X. Wang, G. Shi, On the gelation of graphene oxide, J Phys Chem C 115 (13) (2011) 5545–5551.

[36] H. Kim, C. W. Macosko, Processing-property relationships of polycarbonate/graphene composites, Polymer 50 (15) (2009) 3797–3809.

[37] S. N. Tripathi, R. S. Malik, V. Choudhary, Melt rheology and thermomechanical behavior of poly (methyl methacrylate)/reduced graphene oxide nanocomposites, Polym Advan Technol 26 (12) (2015) 1558–1566.

[38] K. K. Sadasivuni, D. Ponnamma, B. Kumar, M. Strankowski, R. Cardinaels, P. Moldenaers, S. Thomas, Y. Grohens, Dielectric properties of modified graphene oxide filled polyurethane nanocomposites and its correlation with rheology, Compos Sci Technol 104 (2014) 18–25.

[39] L. Yao, Y. Lu, Y. Wang, L. Hu, Effect of graphene oxide on the solution rheology and the film structure and properties of cellulose carbamate, Carbon 69 (2014) 552–562.

[40] M. El Achaby, A. Qaiss, Processing and properties of polyethylene reinforced by graphene nanosheets and carbon nanotubes, Material Design 44 (2013) 81–89.

[41] R. Jalili, S. H. Aboutalebi, D. Esrafilzadeh, R. L. Shepherd, J. Chen, S. Aminorroaya-Yamini, K. Konstantinov, A. I. Minett, J. M. Razal, G. G. Wallace, Scalable one-step wet-spinning of graphene fibers and yarns from liquid crystalline dispersions of graphene oxide: towards multifunctional textiles, Adv Funct Mater 23 (43) (2013) 5345–5354.

[42] M. G. Nasab, M. Kalaee, Epoxy/graphene oxide/liquid polysulfide ternary nano-composites: rheological, thermal and mechanical, characterization, RSC Adv 6 (51) (2016) 45357–45368.

[43] J. K. Dhont, W. J. Briels, Gradient and vorticity banding, Rheol Acta 47 (3) (2008) 257–281.

[44] Y. Tan, Y. Song, Q. Zheng, Hydrogen bonding-driven rheological modulation of chemically reduced graphene oxide/poly (vinyl alcohol) suspensions and its application in electrospinning, Nanoscale 4 (22) (2012) 6997–7005.

[45] K. Yao, H. Tan, Y. Lin, G. Zhang, J. Gong, J. Qiu, T. Tang, H. Na, Z. Jiang, Effect of polystyrene long branch chains on melt behavior and foaming performance of poly (vinyl chloride)/graphene nanocomposites, RSC Adv 4 (109) (2014) 64053–64060.

[46] M. P. Godfrin, F. Guo, I. Chakraborty, N. Heeder, A. Shukla, A. Bose, R. H. Hurt, A. Tripathi, Shear-directed assembly of graphene oxide in aqueous dispersions into ordered arrays, Langmuir 29 (43) (2013) 13162–13167.

[47] R. Shu, Q. Yin, H. Xing, D. Tan, Y. Gan, G. Xu, Colloidal and rheological behavior of aqueous graphene oxide dispersions in the presence of poly (ethylene glycol), Colloid Surface A 488 (2016) 154–161.

[48] J. Wang, L. Shang, Y. Cheng, H. Ding, Y. Zhao, Z. Gu, Microfluidic generation of porous particles encapsulating spongy graphene for oil absorption, Small 11 (32) (2015) 3890–3895.
•This article reports the first microfluidic application of particles made of graphene oxide to remove perfluorooctane sulfonate from water in only two minutes, with an efficiency of 98%.

[49] W. K. Park, H. Kim, T. Kim, Y. Kim, S. Yoo, S. Kim, D. H. Yoon, W. S. Yang, Facile synthesis of graphene oxide in a couette–taylor flow reactor, Carbon 83 (2015) 217–223.

[50] T. S. Tran, S. J. Park, S. S. Yoo, T.-R. Lee, T. Kim, High shear-induced exfoliation of graphite into high quality graphene by taylor–couette flow, RSC Adv 6 (15) (2016) 12003–12008.

[51] H. Zhang, G. Grüner, Y. Zhao, Recent advancements of graphene in biomedicine, J Mater Chem 1 (20) (2013) 2542–2567.

[52] N. M. Bardhan, P. V. Kumar, Z. Li, H. L. Ploegh, J. C. Grossman, A. M. Belcher, G.-Y. Chen, Enhanced cell capture on functionalized graphene oxide nanosheets through oxygen clustering, ACS nano 11 (2017) 1548–1558.